Supplemental Methods

Dissociated cultures

Cortices were dissociated in HBSS plus HEPES with 0.25% trypsin for 15 min and then washed three times for 5 min each with HBSS plus HEPES. The dissociated neurons were then plated on coverslips (22 mm x 22 mm, Fisher) at a density of 5×10^4 cells per well in neurobasal medium (Invitrogen) supplemented with 10 ml l^{-1} Glutamax (Invitrogen), 1 μg ml^{-1} gentamicin (Invitrogen), 20 ml l^{-1} B-27 supplement (Invitrogen) and 50 ml l^{-1} fetal bovine serum (Invitrogen). After 4 h, the medium was replaced with serum-free neurobasal medium. The imaging buffer consisted of 10mM HEPES buffered HBSS + Ca^{2+}+ Mg^{2+} (Invitrogen) containing 125 μM Shield-1 and 0.2% (w/v) F-127 Pluronic (Invitrogen).

COS and Neuron experiments to test FM4/Shield-1 Pulse-Chase system

COS cells were transiently transfected using Effectine (Qiagen) using the manufacturer's suggested protocol. For surface expression assays, COS cells were incubated in the presence or absence of Shield-1 then immunostained after 16 hours of expression for surface and total protein as described in supplemental methods. For long-term timelapse, COS cells were plated on DeltaT (Bioptechs) imaging dishes. After 16 hours of expression, cells were imaged once in imaging solution without Shield-1. Shield-1 was then added and cells were imaged once every 5 minutes for approximately 4 hours. Similar timelapse experiments were also performed with 12 DIV dissociated cortical neurons in an RC-30 chamber (Warner Instruments).

Cytochalasin D Experiments

In order to investigate the effects of disrupting actin 12-14 DIV neuron cultures were exposed to 4 μM Cytochalasin D in imaging buffer for 30-40 min prior to imaging. It was found that this level of exposure was sufficient to disrupt actin significantly within the AIS in approximately 30% of cells. Cells that had been imaged live were then re-imaged from the fixed, stained cultures in order to assess the degree of actin disruption. Once the cells were imaged live the cultures were fixed and stained with Phalloidin-Alexa-647 (Invitrogen). Cells were chosen for analysis that contained actin in a punctate pattern within the AIS indicating that significant disruption of filaments had occurred.

Ankyrin G and Nav II-III-HamCherry Distributions.

To address whether the localization of AnkyrinG within the AIS was altered by the disruption of actin or MyosinVa, we transfected neurons with GFP, incubated for 12 hours under 3 different conditions and subsequently fixed and immunostained for Ankyrin G. Control cells were compared with cells co-transfected with HA-dnMva or cells that were exposed to 8 μM Cytochalasin D for 60 minutes prior to fixing. Similar measurements were also made on the live distributions of $Na_v1.2$ II-III-HAmCherry or $Na_v1.2$ II-III-GFP to assess the effects of HA-dnMVa, co-transfection or exposure to Cytochalasin D.

cDNA constructs

pC_4S_1-FM_4-FCS-hGH (a gift from Ariad Pharmaceuticals) served as the primary source FM4 (4 tandem repeats of FM), which were flanked by Xba1 and Spe1 on the 5' and 3' end, respectively.

Using standard molecular biology methods the cDNA encoding FM4 was inserted downstream of the open reading frame encoding TfR GFP (a gift from G. Banker) to give TfR GFP FM4. The sequence encoding VSVG (a gift from J Lippincott-Schwartz) with the last 28 amino acids truncated was inserted downstream of FM4 to give FM4-VSVGΔC-GFP. The cDNA encoding GluR1 (a gift from R Malinow) was amplified and subcloned upstream of mCherry. GluR1 mCherry was then placed downstream of FM4 to give FM4-GluR1-mCherry. The cDNA encoding mGluR2 (a gift from AM Craig) was inserted downstream of FM4 to give FM4-mGluR2-GFP. To construct FM4-VSVGΔC-GFP-MBD, the sequence encoding melanophilin amino acids 176-201 was amplified and inserted downstream of FM4-VSVGΔC-GFP. The construction of HA-dnMVa was previously described (Lewis et al, 2009). The construction of HA-dnMVI was previously described (Lewis et al, 2011). The cDNA encoding NgCAM (a gift from G Banker) was amplified and subcloned downstream of FM4 and upstream of GFP to give FM4-NgCAM-GFP. $Na_v1.2$ II-III (Garrido et al., 2003) sequence was appended to GFP or HAmCherry with permission from Benedicte Dargent. All open reading frames were expressed under the control of the hCMV promoter.

Immunocytochemistry.

For permeabilized staining of total protein cells were fixed with 4% paraformaldehyde for 5 min,washed with PBS, and blocked with 1% bovine serum albumin, 5% normal goat serum, and 0.1% Triton X-100 in PBS. After blocking, primary antibody was diluted in blocking solution and added for 30–60 min. Secondary antibody was diluted in blocking solution and added for 30 min in the dark. Primary antibody concentrations were as follows: chicken anti-GFP (Aves), 1:1,000; rabbit anti-GFP (BD Biosciences), 1:1,000; mouse anti-HA (Covance), 1:500; rabbit

anti-Ankyrin G (Santa Cruz), 1:1,000; mouse anti-PDI (Thermo Fisher Scientific), 1:100. Secondary antibodies conjugated to Alexa 488, 594, or 647 fluorophores (Invitrogen) were used based on manufacturer's suggestion. For non-permeabilized staining of surface protein primary antibody was diluted in fresh non-serum containing neurobasal medium and was added on the cells for 5–10 min. The cells were then fixed and treated as in the permeabilized staining protocol described above.

Image capture for ADR analysis.

To assay final protein targeting in neurons, cells were transfected using CalPhos with the target construct and HAmCherry in the presence of Shield1. Following 16 hours of expression, cells were fixed, permeabilized and stained for GFP as previously described. ADR analysis was done as before (Lewis et al., 2009) by comparing the expression level in the entire dendrites with expression in the axon distal to the axon initial segment.

Image processing of timelapse data.

To perform background subtraction, we used regression to estimate the background intensity dynamics for each pixel. Given a movie, we first chose a uniform region that best represented the photo bleaching effect on all static structures over time. Then we calculated the average intensity μ_t of this region at each time point $t = 1, \dots, T$, where T is total number of time points. The curve of the average intensities over time (i.e $\mu_1, \mu_2, \dots, \mu_T$) represented the change of overall background intensity with photo bleaching effect of all static structures. For each pixel at each time point, t, we modeled its background intensity, y_t, as a linear function $y_t = a\mu_t + b$ of the overall background intensity μ_t, where a and b are coefficients to be determined. Then the

observed pixel intensity x_t, at time point t, was modeled as the sum of background intensity y_t and a residue r_t that corresponds to the intensity dynamics from the noise and moving objects in image covered by the pixel:

$$x_t = y_t + r_t$$

We used the least squares method to determine optimal a and b. Specifically, we minimize the sum of square of the residues:

$$\min_{a,b} \sum_{t=1}^{T} r_t^2$$

Where $r_t = x_t - y_t = x_t - (a\mu_t + b)$. After calculating the optimal coefficients, denoted as a^* and b^*, we then used $a^* y_t + b^*$ as the estimated background intensity for the pixel, and performed a background subtraction to obtain a background subtracted pixel intensity

$$r_t^* = x_t - (a^* \mu_t + b^*)$$

After the background subtraction for all pixels, we further applied contrast enhancement and Gaussian filtering to the time lapse movie for better visual analysis

2 dimensional plots for vesicle tracking and analysis

To better visualize the vesicle tracks, the distance traveled over time was plotted in each instance where the particle was detected. The distance measurement was approximated in a quasi-1 dimensional manner using the vesicle's current position with respect to the initial point of origin.

Distance traveled = $\sqrt{[(x_i-x_0)^2 + (y_i-y_0)^2]}$

Statistical methods

We compared measurements of the distal borders of the AIS, as defined by endogenous AnkG or the co-expressed Nav1.2 II,III-FP, and following perturbations of the motor or filament, using an unpaired t-test. To determine whether the differences between observed trajectory profiles (proceed, halt, reverse) of vesicles containing various cargos and/or under different conditions were statistically significant, we applied the chi-square test. Note that when comparing the movements of vesicles carrying VSVGΔC-GFP with the three dendritic proteins, or amongst vesicles carrying dendritic proteins, the correct standard for significance is $p < 0.0084$, not $p < 0.05$. The reason for this is that when multiple comparisons are made between members of a group, the Bonferroni correction (Schulerud et al., 1998), which states that the standard for significance is 0.05/n where n is the number of comparisons, must be used. This is particularly true when there is no particular hypothesis, as otherwise in one experiment in 20 a significant result would be found where none existed. For our experiments, we measured movements of 4 types of vesicles in total, and thus there are 6 possible comparisons (3 comparisons to the non-specifically localized protein and 3 among the dendritic proteins).

References

Garrido, J.J., Giraud, P., Carlier, E., Fernandes, F., Moussif, A., Fache, M.P., Debanne, D., and Dargent, B. (2003). A targeting motif involved in sodium channel clustering at the axonal initial segment. Science *300*, 2091-2094.

Lewis, T.L., Jr., Mao, T., Svoboda, K., and Arnold, D.B. (2009). Myosin-dependent targeting of transmembrane proteins to neuronal dendrites. Nat Neurosci *12(5)*, 568-576.

Schulerud, H., Kristensen, G.B., Liestol, K., Vlatkovic, L., Reith, A., Albregtsen, F., and Danielsen, H.E. (1998). A review of caveats in statistical nuclear image analysis. Anal Cell Pathol *16*, 63-82.

Supplemental Figures

Figure S1 Demarcation of AIS. (Associated with Figure 2). (**A**) Neuron expressing $Na_v1.2$ II-III-HAmCherry, which exhibits enrichment at the AIS. (**B**) Fluorescence intensity versus distance. The AIS distal border is defined as the point at which staining is 50% of the peak value. (**C**) Magnification of boxed region in (**A**). Note that the distal AIS border in (**A**-**C**) is marked by a dashed red line. (**D**) Classification of vesicle paths using standardized distal borders of 15 or 20 μm for TfR and VSVGΔC result in strikingly similar trajectory profiles when compared to the criteria defined in (**B**), 1/2 max AIS-FL, and used throughout.

Figure S2 Analysis of vesicles containing TfR, VSVGΔC, and NgCAM in representative cells. (Associated with Figure 3) (**A**, **B, C**) Representative cells showing paths taken by vesicles carrying TfR-GFP-FM4 following entry into axons or dendrites. (**D**) Axon and dendrite scatter plots showing the ratio of the number of vesicles carrying TfR-GFP-FM4 that proceed versus the number that halt or reverse for the cells in (**A**-**C**). (**E**, **F, G**) Representative cells showing paths taken by vesicles carrying FM4-VSVGΔC-GFP following entry into axons or dendrites. (**H**) Scatter plots showing the ratio of the number of vesicles carrying FM4-VSVGΔC-GFP that proceed versus the number that halt or reverse for the cells in (**E**-**G**). (**I**, **J, K**) Representative cells showing paths taken by vesicles carrying FM4-NgCAM-GFP following entry into axons or dendrites. (**L**) Scatter plots showing the ratio of the number of vesicles carrying FM4-NgCAM-GFP that proceed versus the number that halt or reverse for the cells in (**I**-**K**). Dashed red line marks the distal border of the AIS. Scale bar is 5 μm.

Figure S3 Analysis of vesicles containing GluR1 and mGluR2 in representative cells. (Associated with Figure 4) (**A**, **B, C**) Representative cells showing paths taken by vesicles

carrying FM4-GluR1-mCherry following entry into axons or dendrites. (**D**) Axon and dendrite scatter plots showing the ratio of the number of vesicles carrying FM4-GluR1-mCherry that proceed versus the number that halt or reverse for the cells in (**A**-**C**). (**E**, **F, G**) Representative cells showing paths taken by vesicles carrying FM4-mGluR2-GFP following entry into axons or dendrites. (**H**) Scatter plots showing the ratio of the number of vesicles carrying FM4-mGluR2-GFP that proceed versus the number that halt or reverse for the cells in (**E**-**G**). Note that each data point refers to a single cell. Plots of distance traveled versus time indicate that most vesicles in the axon carrying either FM4-GluR1-mCherry (**I**) or FM4-mGluR2-GFP (**L**) tend to halt or reverse within AIS. Plots of distance traveled versus time for vesicles carrying either FM4-GluR1-mCherry (**J**) or FM4-mGluR2-GFP (**M**) within dendrites. (**K**, **N**) Scatter plots showing the ratio of the number of vesicles carrying either FM4-GluR1-mCherry or FM4-mGluR2-GFP that proceed versus the number that halt or reverse. In axons the two types of vesicles behave similarly to each other and to those carrying TfR-GFP-FM4. In dendrites vesicles carrying FM4-GluR1-mCherry or FM4-mGluR2-GFP behave similarly to each other. Dashed red line marks the distal border of the AIS.

Figure S4. Analysis of vesicles containing TfR upon disrupting actin filaments or myosin motors, and of vesicles containing VSVGΔC-MBD, in representative cells. (Associated with Figure 5) (**A**, **B, C**) Representative cells showing paths taken by vesicles carrying TfR-GFP-FM4 following entry into axons or dendrites in cells exposed to 4 μM cytochalasin D for 80 minutes. (**D**) Scatter plot showing the ratio of the number of vesicles carrying TfR-GFP-FM4 that proceed versus the number that halt or reverse for the cells in (**A**-**C**). (**E**, **F, G**) Representative cells showing paths taken by vesicles carrying TfR-GFP-FM4 following entry into axons or dendrites in cells co-expressing HA-dnMVa. (**H**) Scatter plots showing the ratio of the number of vesicles

carrying TfR-GFP-FM4 that proceed versus the number that halt or reverse for the cells in (**E-G**). (**I**, **J, K**) Representative cells showing paths taken by vesicles carrying TfR-GFP-FM4 following entry into axons or dendrites in cells co-expressing HA-dnMVI. (**L**) Scatter plots showing the ratio of the number of vesicles carrying TfR-GFP-FM4 that proceed versus the number that halt or reverse for the cells in (**I-K**). (**M, N, O**) Representative cells showing paths taken by vesicles carrying FM4-VSVGΔC-GFP-MBD following entry into axons or dendrites. (**P**) Scatter plots showing the ratio of the number of vesicles carrying FM4-VSVGΔC-GFP-MBD that proceed versus the number that halt or reverse for the cells in (**M-O**). Dashed red line marks the distal border of the AIS. Scale bar is 5 μm.

Figure S5 Disrupting actin filaments or Myosin Va function does not affect AIS. (Associated with Figure 6) **(A)** Distance from the cell body at which the staining of Ankyrin G is half the maximum (Ankyrin G ½max) is not significantly different in control cells versus cells co-expressing HA-dnMva or in cells exposed to cytochalasin D. (Ankyrin G $½max_{Control}$ = 13 ± 1 μm (n=13), Ankyrin G $½max_{HA\text{-}dnMVa}$ = 13 ± 1 μm (n=15), Ankyrin G $½max_{cytoD}$ = 16 ± 1 (n=14); p > 0. 14, t-test. (**B**) Similar measurements for $Na_v1.2$ II-III-HAmCherry ($Na_v1.2$ II-III-$HAmCherry_{Control}$ = 18 ± 3 (n=7), $Na_v1.2$ II-III-$HAmCherry_{HA\text{-}dnMVa}$ = 15 ± 2 (n=8), $Na_v1.2$ II-III-$HAmCherry_{cyto\ D}$ = 14 ± 2 (n=7). Error bars represent SEM.

Figure S6 Measurement of axon to dendrite ratios. (Associated with Figure 7) Steady-state localization of FM4-fused proteins in the presence of Shield-1. In a neuron expressing (**A**) FM4-VSVGΔC-GFP-MBD and (**B**) HA-mCherry in the presence of Shield-1 FM4-VSVGΔC-GFP-MBD localized specifically to the somatodendritic region and was absent from the axon, whereas HAmCherry localized nonspecifically. In a neuron expressing (**C**) TfR-GFP-FM4, and (**D**) HA-

dnMVa in the presence of Shield-1 both proteins localized nonspecifically. In a neuron expressing (**E**) TfR-GFP-FM4, and (**F**) HA-mCherry in the presence of 1μM cytochalasin D and Shield-1 TfR-GFP-FM4 localized non-specifically in a similar manner to HAmCherry. (**G**) The axon-to-dendrite ratios (ADRs; see methods) of FM4-fused proteins. ($ADR_{FM4\text{-}VSVG\Delta C\text{-}GFP}$ = 1.1 +/- 0.2 (n = 10); $ADR_{TfR\text{-}GFP\text{-}FM4}$ = 0.24 +/- 0.03(n = 10); $ADR_{TfR\text{-}GFP\text{-}FM4 + Cyto\ D}$ = 0.9 +/- 0.1 (n = 11); $ADR_{FM4\text{-}VSVG\Delta C\text{-}MBD\text{-}GFP}$ = 0.27 +/- 0.02 (n = 10); $ADR_{TfR\text{-}GFP\text{-}FM4 + HA\text{-}dnMVa}$ = 0.97 +/- 0.06 (n = 10). Error bars denote SEM. Arrows point to the axon; arrowheads to the axon initial segment. Insets show staining for Ankyrin G, used to identify the axon. Scale bars, 10 μm.

Supplemental Movies

Movie 1 Figure 2-associated movie.

Representative cell showing tracks of TfR-GFP-FM4-containing vesicles upon departure from the Golgi and entry into the axon or dendrites. Note that the Golgi is outlined in yellow and the axon is marked with an arrowhead.

Movie 2 Figure 3-associated movie.

Representative cell showing tracks of TfR-GFP-FM4-containing vesicles following entry into the axon or dendrites. Note that axon is marked with a red arrowhead and yellow line marks the border of the AIS.

Movie 3 Figure 3-associated movie.

Representative cell showing tracks of FM4-VSVGΔC-GFP-containing vesicles following entry into the axon or dendrites.

Movie 4 Figure 4-associated movie.

Representative cell showing tracks of FM4-NgCAM-GFP-containing vesicles following entry into the axon or dendrites.

Movie 5 Figure 4-associated movie.

1. Representative cell showing tracks of FM4-GluR1-mCherry-containing vesicles following entry into the axon or dendrites. 2. Representative cell showing tracks of FM4-mGluR2-GFP-containing vesicles following entry into the axon or dendrites.

Movie 6 Figure 5-associated movie.

Representative cell exposed to 4 μM cytochalasin D for 80 minutes showing tracks of TfR-GFP-FM4-containing vesicles following entry into the axon or dendrites.

Movie 7 Figure 6-associated movie.

1. Representative cell coexpressing HA-dnMVa showing tracks of TfR-GFP-FM4-containing vesicles following entry into the axon or dendrites. 2. Representative cell coexpressing HA-dnMVI showing tracks of TfR-GFP-FM4-containing vesicles following entry into the axon or dendrites.

Movie 8 Figure 6-associated movie.

Representative cell showing tracks of FM4 FM4-VSVGΔC-GFP-MBD-containing vesicles following entry into the axon or dendrites.

Figure S1

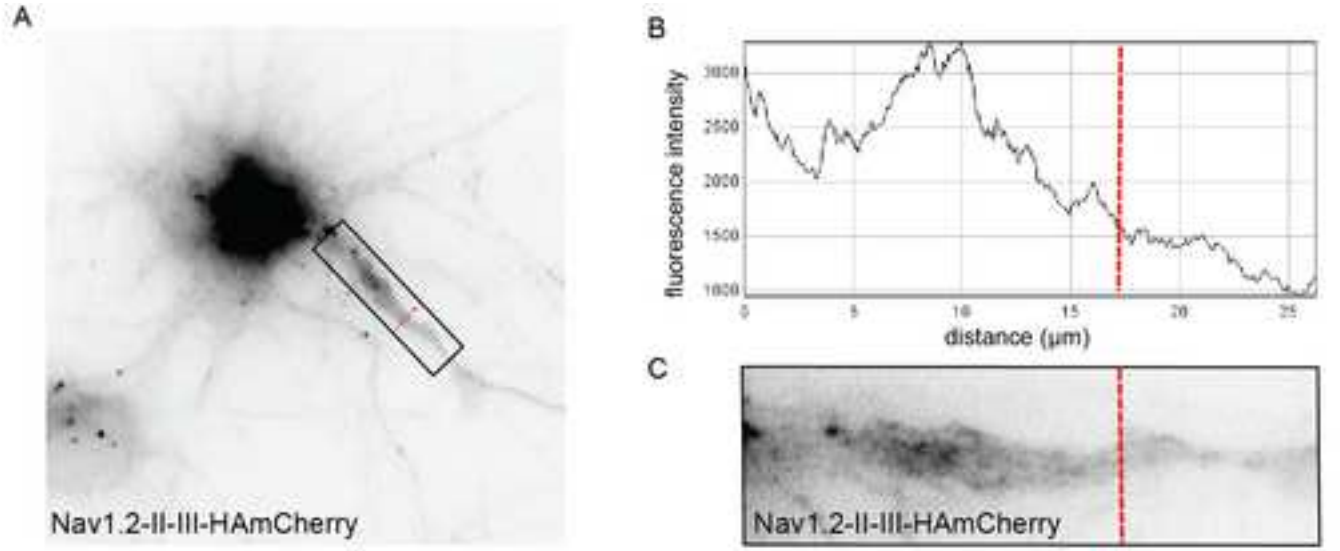
A
Nav1.2-II-III-HAmCherry
B
fluorescence intensity
distance (µm)
C
Nav1.2-II-III-HAmCherry

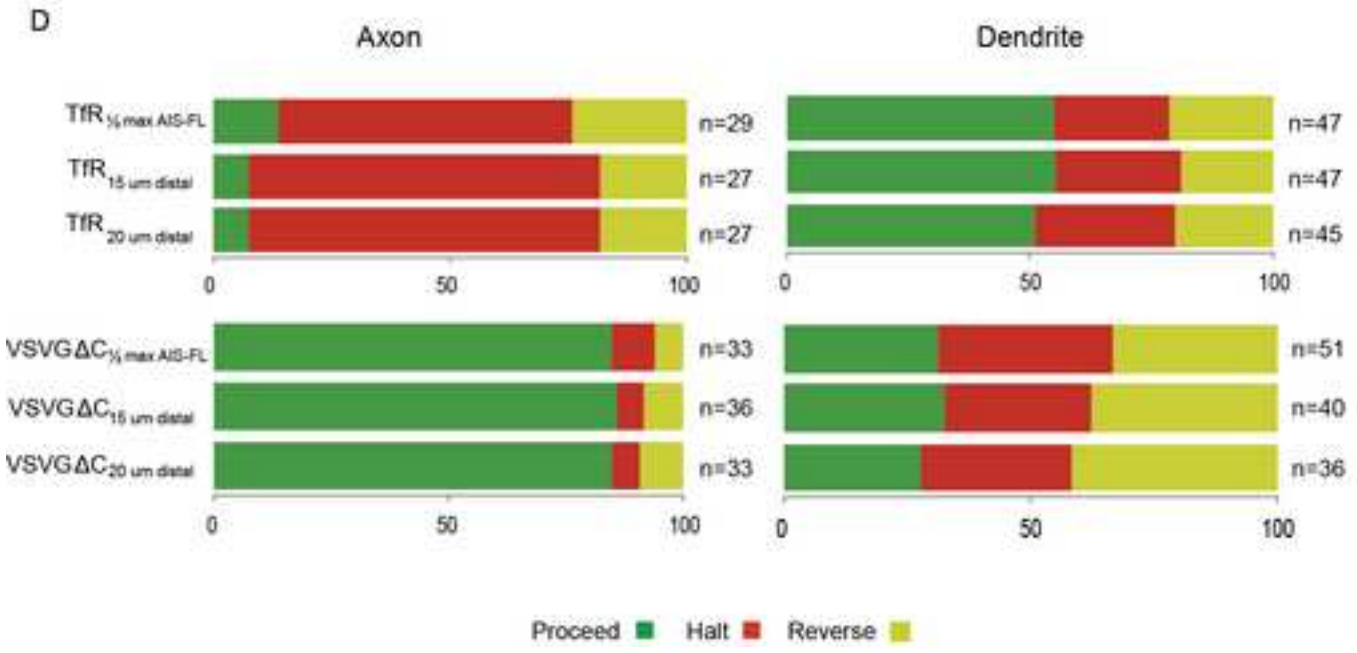
D
Axon
Dendrite
TfR ½ max AIS-FL
TfR 15 um distal
TfR 20 um distal
VSVGΔC ½ max AIS-FL
VSVGΔC 15 um distal
VSVGΔC 20 um distal
n=29
n=27
n=27
n=47
n=47
n=45
n=33
n=36
n=33
n=51
n=40
n=36
0
50
100
Proceed
Halt
Reverse

Figure S2

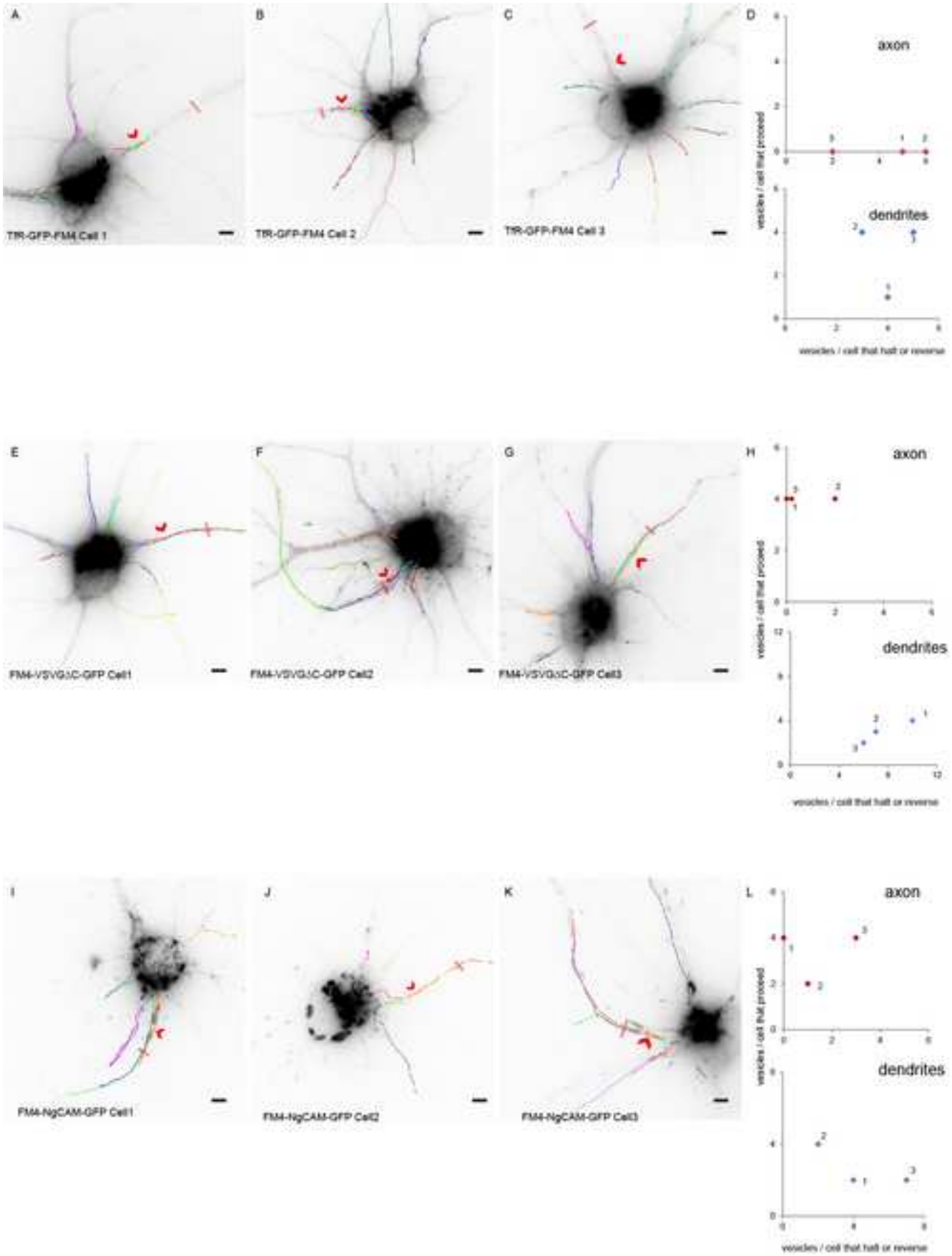
A
TfR-GFP-FM4 Cell 1
B
TfR-GFP-FM4 Cell 2
C
TfR-GFP-FM4 Cell 3
D
axon
dendrites
vesicles / cell that halt or reverse
E
FM4-VSVGΔC-GFP Cell1
F
FM4-VSVGΔC-GFP Cell2
G
FM4-VSVGΔC-GFP Cell3
H
axon
dendrites
vesicles / cell that halt or reverse
I
FM4-NgCAM-GFP Cell1
J
FM4-NgCAM-GFP Cell2
K
FM4-NgCAM-GFP Cell3
L
axon
dendrites
vesicles / cell that halt or reverse

Figure S3

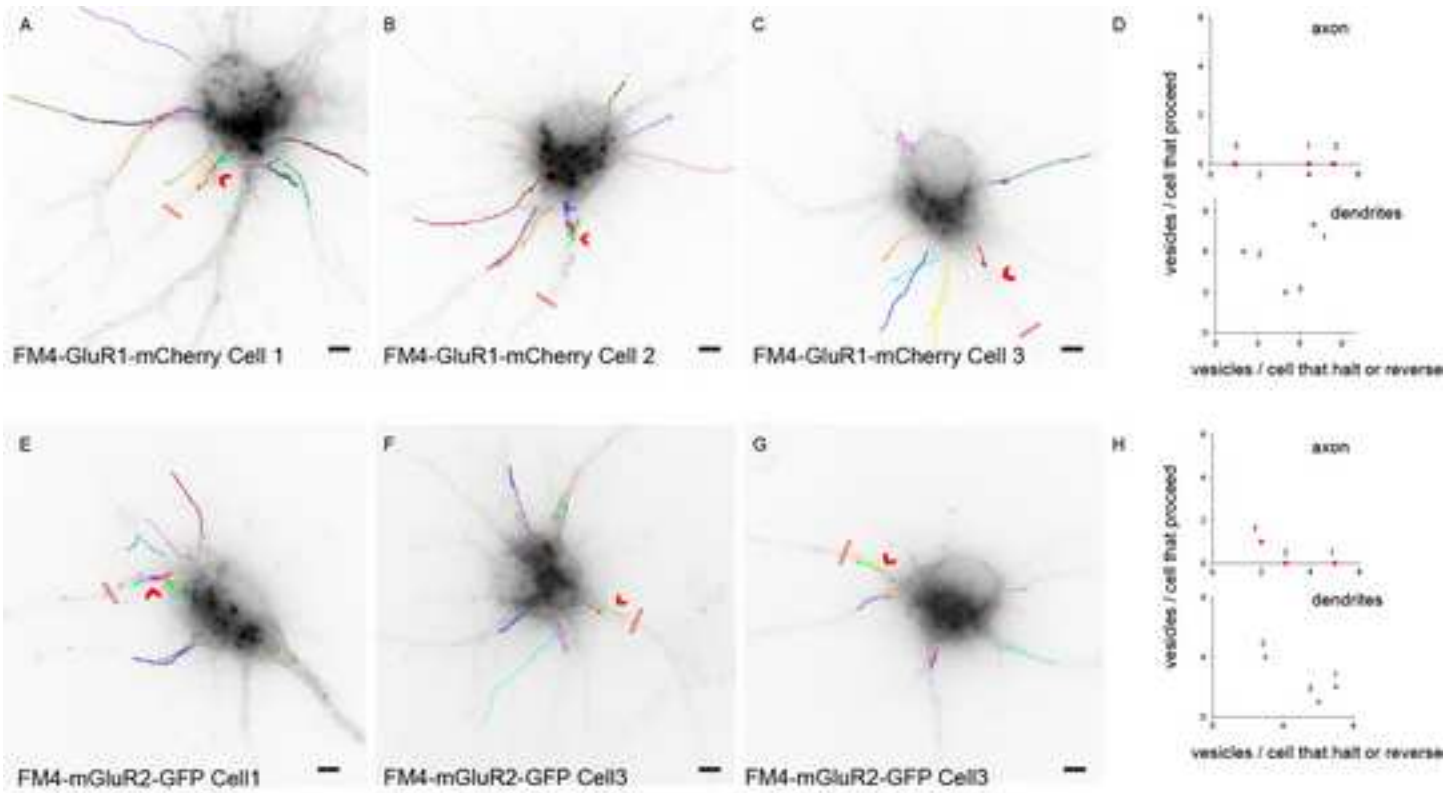
A
B
C
D
FM4-GluR1-mCherry Cell 1
FM4-GluR1-mCherry Cell 2
FM4-GluR1-mCherry Cell 3
axon
dendrites
vesicles / cell that proceed
vesicles / cell that halt or reverse
E
F
G
H
FM4-mGluR2-GFP Cell1
FM4-mGluR2-GFP Cell3
FM4-mGluR2-GFP Cell3
axon
dendrites
vesicles / cell that proceed
vesicles / cell that halt or reverse

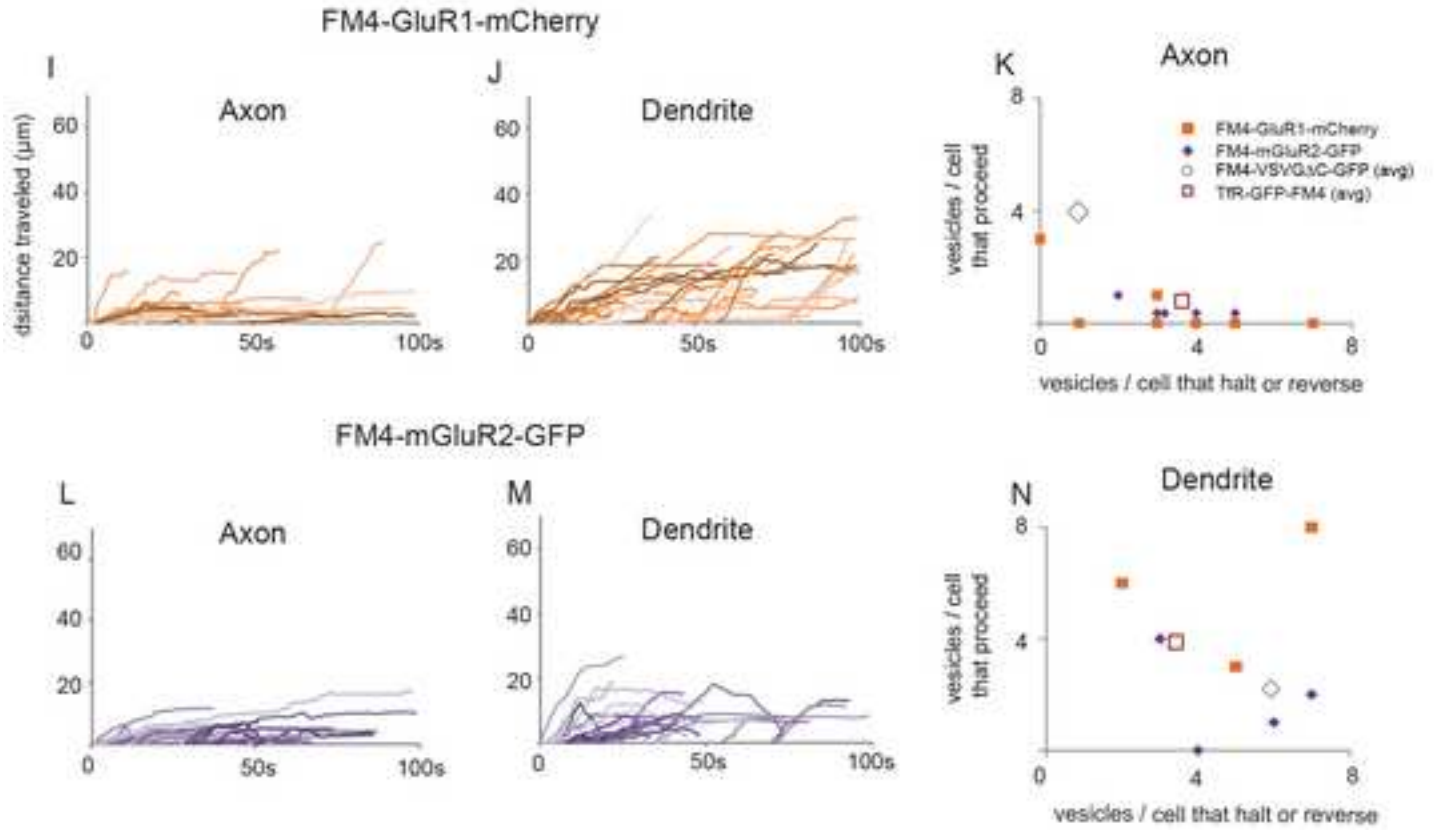
FM4-GluR1-mCherry
I
Axon
J
Dendrite
K
Axon
distance traveled (µm)
60
40
20
0
50s
100s
8
4
vesicles / cell that proceed
FM4-GluR1-mCherry
FM4-mGluR2-GFP
FM4-VSVGΔC-GFP (avg)
TfR-GFP-FM4 (avg)
vesicles / cell that halt or reverse
FM4-mGluR2-GFP
L
Axon
M
Dendrite
N
Dendrite

Figure S4

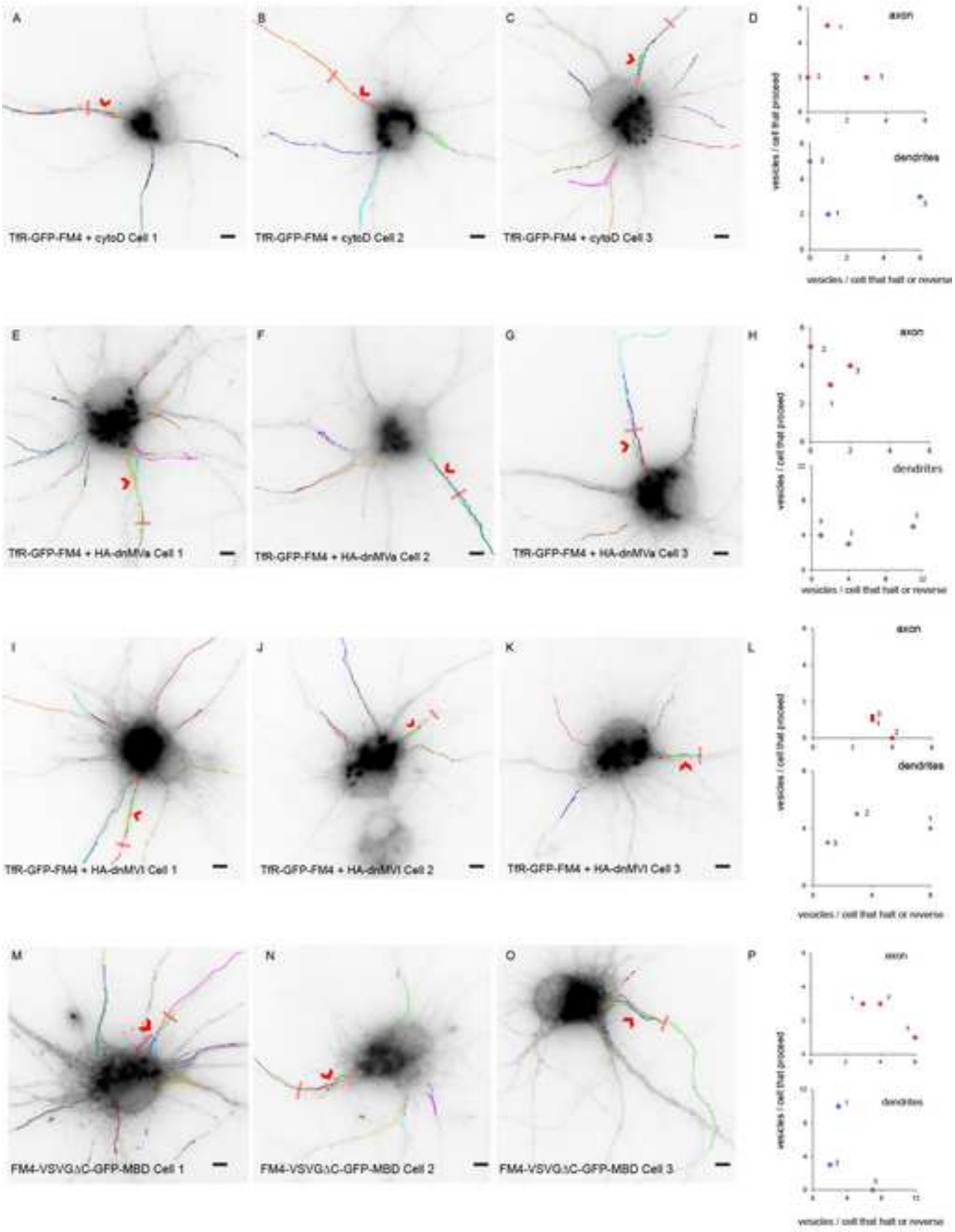
A
TfR-GFP-FM4 + cytoD Cell 1
B
TfR-GFP-FM4 + cytoD Cell 2
C
TfR-GFP-FM4 + cytoD Cell 3
D
axon
dendrites
vesicles / cell that proceed
vesicles / cell that halt or reverse
E
TfR-GFP-FM4 + HA-dnMVa Cell 1
F
TfR-GFP-FM4 + HA-dnMVa Cell 2
G
TfR-GFP-FM4 + HA-dnMVa Cell 3
H
axon
dendrites
vesicles / cell that proceed
vesicles / cell that halt or reverse
I
TfR-GFP-FM4 + HA-dnMVI Cell 1
J
TfR-GFP-FM4 + HA-dnMVI Cell 2
K
TfR-GFP-FM4 + HA-dnMVI Cell 3
L
axon
dendrites
vesicles / cell that proceed
vesicles / cell that halt or reverse
M
FM4-VSVGΔC-GFP-MBD Cell 1
N
FM4-VSVGΔC-GFP-MBD Cell 2
O
FM4-VSVGΔC-GFP-MBD Cell 3
P
axon
dendrites
vesicles / cell that proceed
vesicles / cell that halt or reverse

Figure S5

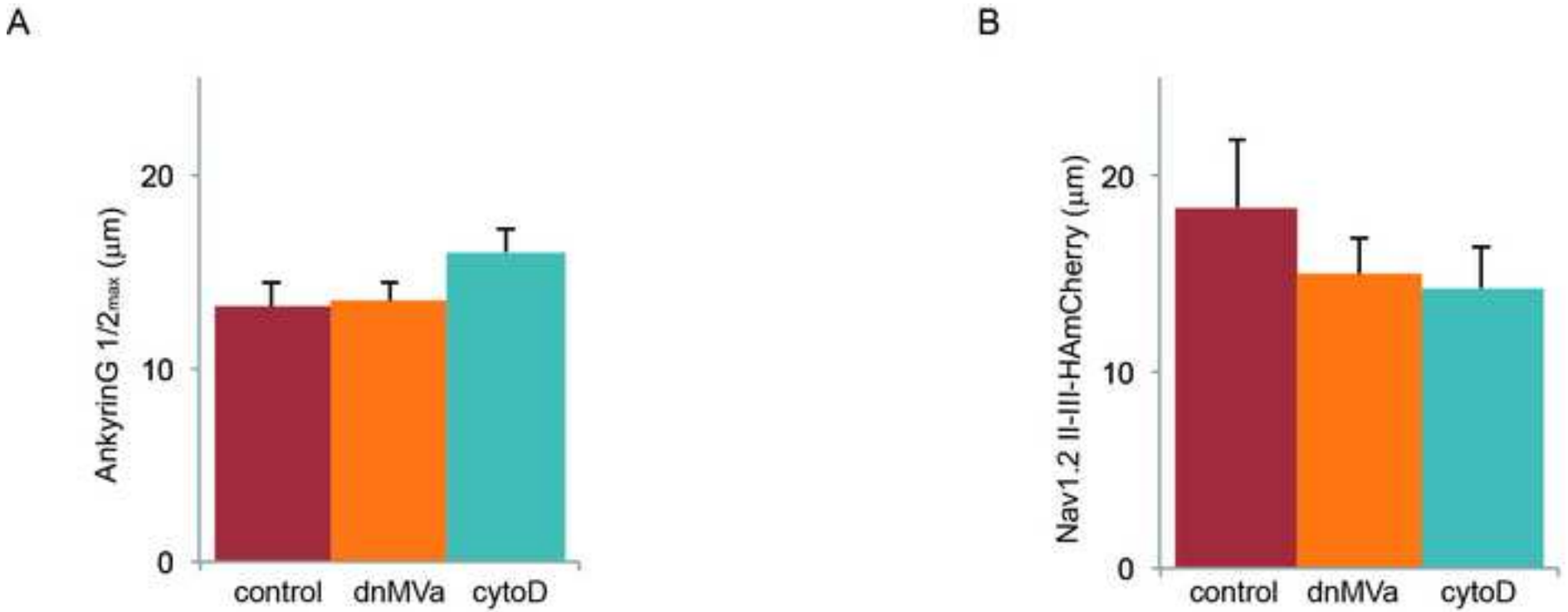
A
AnkyrinG 1/2max (µm)
20
10
0
control
dnMVa
cytoD
B
Nav1.2 II-III-HAmCherry (µm)
20
10
0
control
dnMVa
cytoD

Figure S6

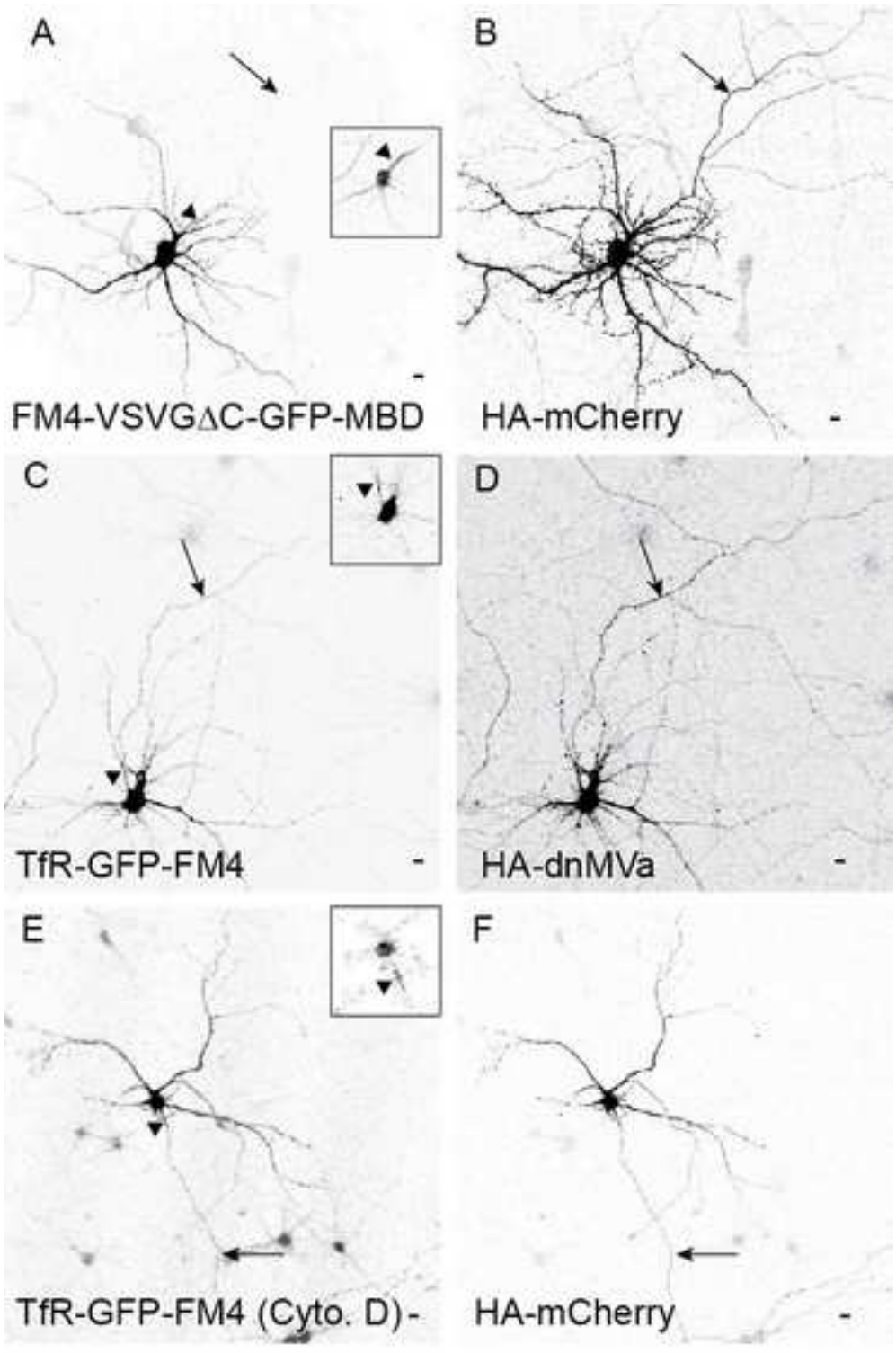
A
FM4-VSVGΔC-GFP-MBD
B
HA-mCherry
C
TfR-GFP-FM4
D
HA-dnMVa
E
TfR-GFP-FM4 (Cyto. D)
F
HA-mCherry
G
ADR
FM4-VSVGΔC-GFP
TfR-GFP-FM4
TfR-GFP-FM4 + Cyto D
FM4-VSVGΔC-GFP-MBD
TfR-GFP-FM4 + HA-dnMvA
0
0.5
1.0